Naphthazarin-Polycyclic Conjugated Hydrocarbons and Iptycenes

Naphthazarin-Polycyclic Conjugated Hydrocarbons and Iptycenes

Cagatay Dengiz[§], Sarah P. Luppino[§], Gregory D. Gutierrez, and Timothy M. Swager*

Department of Chemistry, Massachusetts Institute of Technology, Cambridge, MA 02139, United States

ABSTRACT. The synthesis of a set of naphthazarin-containing polycyclic conjugated hydrocarbons is described herein. Sequential Diels–Alder reactions on a tautomerized naphthazarin core were employed to access the final conjugated systems. Complete conjugation across the backbone can be achieved through complexation with BF_2, as observed by ^1H NMR analysis and UV/vis spectroscopy. Precise synthetic control over the degree of oxidation of naphthazarin quinone Diels–Alder adduct **10** is additionally demonstrated, and enables us to direct its subsequent reactivity. Finally, this work serves to demonstrate the potential for naphthazarin as a building block in the synthesis of novel organic electronic materials.

Keywords: naphthazarin / Diels–Alder reactions / phenylene-containing oligoacenes / BF_2-complex / polycyclic conjugated hydrocarbons / iptycenes

INTRODUCTION

Polycyclic conjugated hydrocarbons are organic small molecules of interest as active materials in electronic and optoelectronic devices. Acenes, such as pentacene and triisopropylsilyl-pentacene (TIPS-pentacene), are among the top performers in organic field effect transistors (OFETs),[1,2] and while they have achieved significant milestones,[3] considerable efforts remain focused on the design and synthesis of new classes of compounds to achieve a desired boost in performance and material stability.

To this end, synthetic chemists have explored structural modifications to the acene core to achieve improved stability, processibility, and electronic properties. Strategies include appending bulky or electron-withdrawing substituents,[1,4] or including heteroatoms into the core acene unit, such as in the synthesis of anthradithiophenes or azaacenes.[1,5–13] Other efforts explore a redesign of the bonding architecture of the core molecule, such as through the incorporation of formally antiaromatic cyclobutadiene units, present in [N]phenylenes and phenylene-containing oligoacenes (POAs).[14–19] Alternation of cyclobutadiene units with either benzene ([N]phenylenes) or acene units (POAs) results in localized conjugation along the molecular backbone, which can improve chromophore stability.[15,16]

Key synthetic approaches to building acene or acene-like small molecules include sequential Diels–Alder reactions,[16,20,21] cross-coupling methods,[6,22] or the [2+2+2] methodology used by Vollhardt and coworkers to synthesize extended [N]phenylenes.[15]

In this study, we capitalize on the ability of naphthazarin (1,4-dihydroxy-5,8-naphthaquinone)[23–25] to act as a bifunctional Diels–Alder reagent to access new iptycene and POA molecules in a convergent manner. Examples of target structures are presented in Figure 1. Naphthazarin has the ability to react twice as a dienophile,[26]

which can be achieved *via* oxidation and tautomerization of the initial Diels–Alder adduct to unmask a second dienophile equivalent on the opposite side of the naphthazarin core. This makes it an appealing building block to convergently synthesize multi-ring systems. Historically, naphthazarins have been utilized predominantly in the construction of anthracyclinones,[23–27] and in this study we intend to demonstrate its further potential as a useful building block in the synthesis of organic electronic materials.

We also demonstrate that the naphthazarin-derived Diels–Alder adducts presented herein can coordinate to two BF_2 groups to form conjugated electron-deficient complexes.[28,29] These types of materials may prove useful as electron-transporting materials and n-type semiconductors.[28,29] To this end, we report the synthesis and spectroscopic properties of a set of triptycene, pentiptycene, and POA naphthazarin-based structures (Figure 1), as well as a proof-of-concept demonstration of their complexation with BF_3-OEt_2.

Figure 1. Three of the naphthazarin-containing target molecules synthesized in this study.

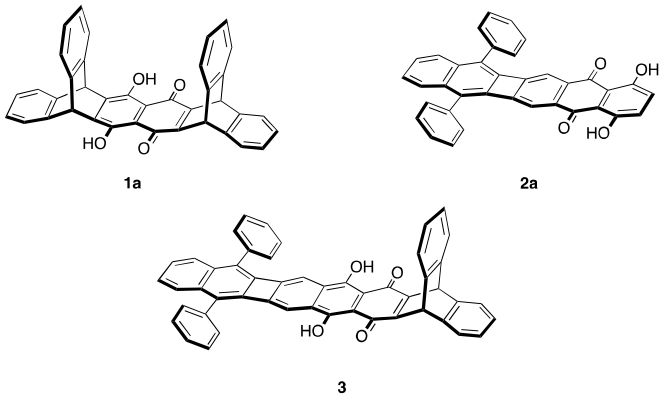

RESULTS AND DISCUSSION

Synthesis of naphthazarin triptycene derivatives 7a–d. Triptycene compounds **7a–d** were accessed through an initial [4+2] Diels–Alder cycloaddition reaction of

naphthazarin (**5**) with a corresponding anthracene (**4a**–**d**) to furnish mono-cycloadducts **6a**–**d**, followed by oxidation to the target triptycene intermediates **7a**–**d** (Scheme 1).

Scheme 1. Synthesis of naphthazarin triptycenes **7a**–**d** and pentiptycenes **1a**–**d**.

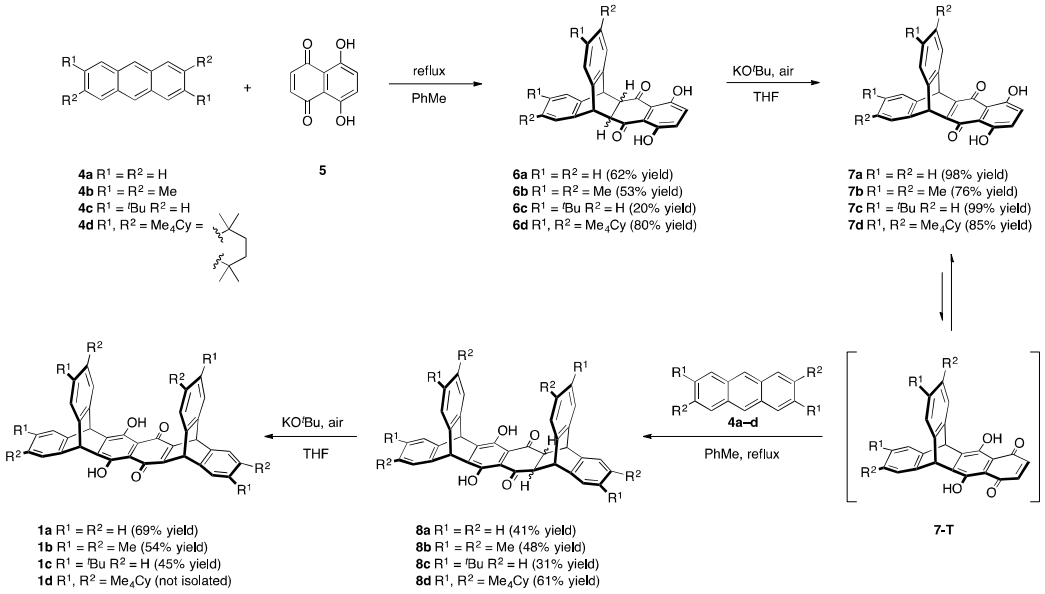

Formation of cycloadducts **6a**–**d** occurred in moderate to good yields (20–80%). Oxidation of **6a**–**d** in the presence of air and excess of KO^{t}Bu produced naphthazarin triptycenes **7a**–**d** in nearly quantitative yields. Reactivity of the anthracene precursors with naphthazarin varies, and we observe anthracene **4d** reacting in the highest yield, likely due to its more electron-rich character relative to the other selected anthracenes.

Single crystals of **6b**, **7a**, and **8a** suitable for X-ray crystallography were obtained by slow evaporation from CH_2Cl_2/*n*-hexane at 25 ^oC (Figures 2 and S1–3, Supporting Information). Although DFT calculations support the tetrasubstituted quinone tautomer **7a** as the more thermodynamically stable isomer,[23] the crystal structure of **7a** was elucidated as tautomer **7a-T**. Calculations at the B3LYP/6-31G(d) level showed that the energy difference between structures **7a** and **7a-T** is 1.05

kcal/mol. (For further details on the computational investigations, see the Supporting Information.)

Figure 2. Three X-ray crystal structures of iptycenes **6b**, **7a**, and **8a**.

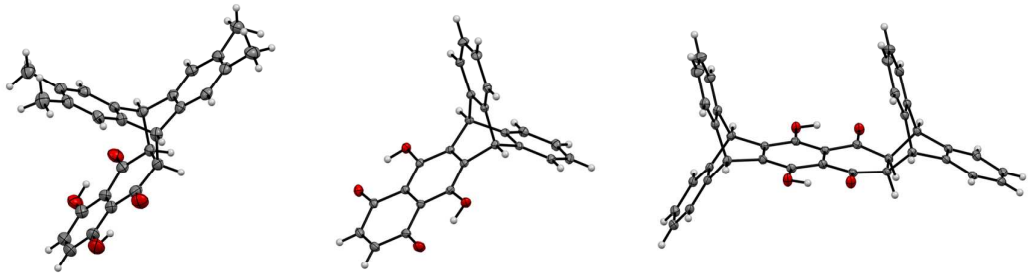

6b **7a** **8a**

Synthesis of naphthazarin pentiptycene compounds 1a–d. Naphthazarin-based cycloadducts are known to tautomerize to expose the quinone-based dienophile (**7-T**), which can undergo a second cycloaddition reaction with a diene.[26] Upon heating, we observed a second equivalent of **4a**–**d** to undergo a [4+2] cycloaddition with **7a**–**d** to yield double-cyloadducts **8a**–**d** in 31–61% yields (Scheme 1).

Similar to the conversion observed from **6a**–**d** to **7a**–**d**, we found that KO^{t}Bu enolized cycloadducts **8a–c** and, in the presence of air, cleanly transformed them into **1a–c** in excellent yield. This method of oxidation is very mild, and enables us to access a portfolio of functionalized naphthazarin pentiptycenes[30] with varying degrees of internal free volume.[31] Isolation of pentiptycene **1d**, however, was not possible. Although we observed characteristic changes in color that signified conversion of **8d** to **1d** (from yellow to dark blue upon addition of KO^{t}Bu, then to dark red after work-up), our attempts to isolate **1d** were unsuccessful as a result of the limited solubility and unexpected decomposition of the product. (See Figure S46 for the UV/vis spectrum of the final reaction mixture.)

Synthesis of naphthazarin phenylene-containing-oligoacene compounds 2a–b and 3. We next hypothesized that the Diels–Alder reactivity of the naphthazarin core

could be extended to a synthetic approach to access novel POAs.[16,19] Naphthazarin presents an opportunity to incorporate an electron-deficient acene unit into the POA backbone, in particular when complexed with BF_2. The naphthazarin motif also provides functional handles for further synthetic manipulation or complexation to metals[32,33] and boron moieties.[28,29]

To synthesize naphthazarin-derived POAs, we utilized diene **9**, which can be accessed in two steps according to literature procedures.[16,19,34–39] Diene **9** was reacted with naphthazarin (**5**) to furnish mono-adduct **10** in 49% yield (Scheme 2). Interestingly, X-ray crystallographic analysis of compound **10** shows a *trans* arrangement of the hydrogen atoms located at the adduct site (Figure S4 in the SI). This is in stark contrast to the expected stereochemistry of Diels–Alder cycloaddition products, as the *exo* and/or *endo* product is often observed, and the resultant placement of hydrogen atoms in space depends on this product ratio.[40] The *trans* relationship in the crystal structure of **10** could signify that the operative mechanism of reaction is, in fact, step-wise instead of a true concerted cycloaddition. Alternatively, the *trans* relationship may be due to epimerization resulting from enolization at the α-carbon that occurs following a conventional *cis* [4+2] cycloaddition. An explanation is that the hydrogen-bonding between the hydroxyl groups and the ketones of the naphthazarin core increases the likelihood of enolization at the α-carbons, and, for sterically-induced reasons, the hydrogen atoms end up *trans* to one another. While we observe a *trans* relationship for compound **10** by X-ray analysis, we detect the presence of three isomers by NMR (Figure S84 in the SI), leading us to conclude that the *trans* product is likely present alongside the *endo* and *exo* adducts.

Scheme 2. Targeted synthesis of naphthazarin POA mono-adducts **2a**–**b**.

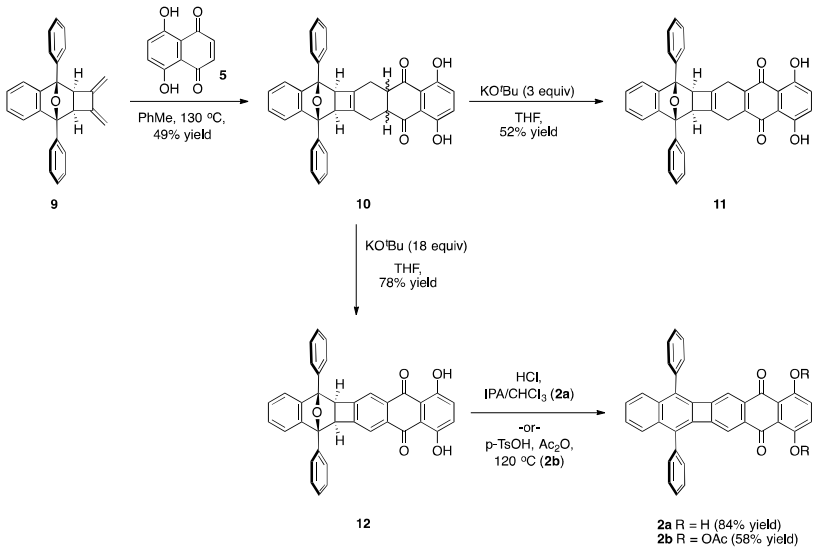

With **10** in hand, we next unmasked dienophile **11-T** to enable further Diels–Alder reactivity (Scheme 3), and found an interesting dependence on the equivalents of KO^{t}Bu used. By adjusting the amount of KO^{t}Bu and reaction time, we were able to effectively tune the level of oxidation to produce either partially-oxidized product **11** or fully-oxidized product **12** (Scheme 2).[26] This capability is significant, as we found that only partially-oxidized **11** is able to further tautomerize *in situ* to produce **11-T**, which brandishes an external-facing dienophile. Fully-oxidized **12** contains an additional aromatic ring that stabilizes and "locks" the internal 9,10-quinone in place. Here, we found that when mono-adduct **10** was reacted with only three equivalents of KO^{t}Bu for a short period of time (five minutes), we were able to achieve the partially oxidized product **11** in 52% yield. When reacted in significant excess and for extended periods of time, the fully oxidized product **12** became the major or sole product (18 equiv., 78% yield). X-ray crystal structures of **10**–**12** are shown in Figures S4–S6 in the SI.

Fully-oxidized **12** can be converted to target compound **2a** in 84% yield through hydrolysis of the bridging oxygen when exposed to an acidic solution of hydrochloric acid in chloroform and isopropyl alcohol.[41] Poor solubility of **2a**

prevented acquisition of a ^{13}C NMR spectrum. An alternative target was found in **2b**, which proved more soluble than **2a**, and can be obtained through conversion from **12** (58% yield) or from **2a** (49% yield) using *p*-TsOH/Ac_2O.

Scheme 3. Targeted synthesis of POA double-adduct **14**.

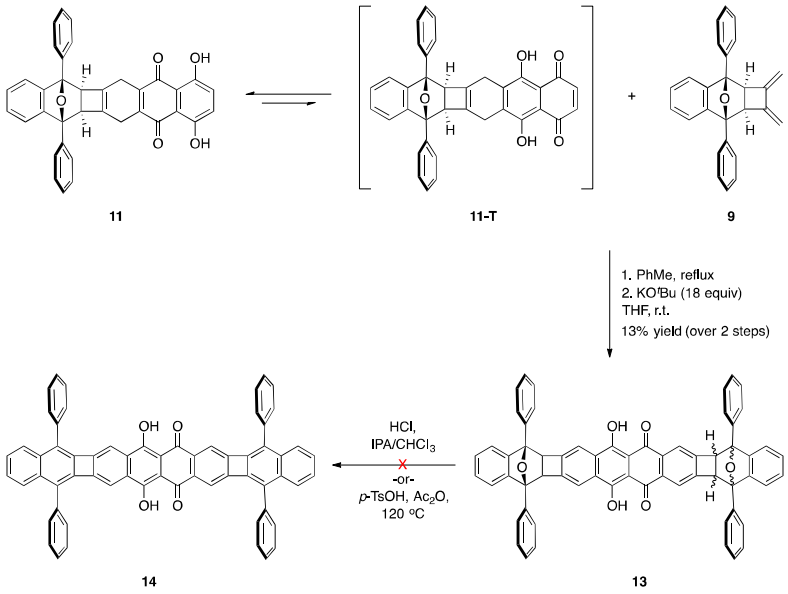

We next induced tautomerization of partially-oxidized **11**, and reacted the *in situ*-generated **11-T** dienophile with diene **9** for a second cycloaddition reaction. Overall, Diels–Alder reaction of **11-T** with diene **9** and subsequent oxidation with KO^{t}Bu in the presence of air yielded **13** in 13% yield. Unfortunately, multiple attempts to convert **13** to the final symmetrical POA double-adduct **14** failed. The challenges we faced in isolating **14** were likely due to poor solubility, as was similarly encountered with pentiptycene **1d** and POA mono-adduct **2a**. We did observe consumption of **13** upon exposure to acid and were able to detect **14** by MALDI-TOF mass spectrometry (see Figure S112). However, the reaction largely produced a substantial amount of insoluble material that we were unable to isolate for full characterization.

To circumvent these problems, we redesigned our synthetic plan and instead targeted compound **3** (Scheme 4). We hypothesized that the non-planar triptycene end-group of **3** would eliminate the aforementioned solubility and aggregation issues.[31] We attempted to react the *in situ* generated **11-T** dienophile with one equivalent of anthracene **4a**, but were only able to observe trace amounts of product by TLC.

Scheme 4. Targeted synthesis of iptycene-POA **3**.

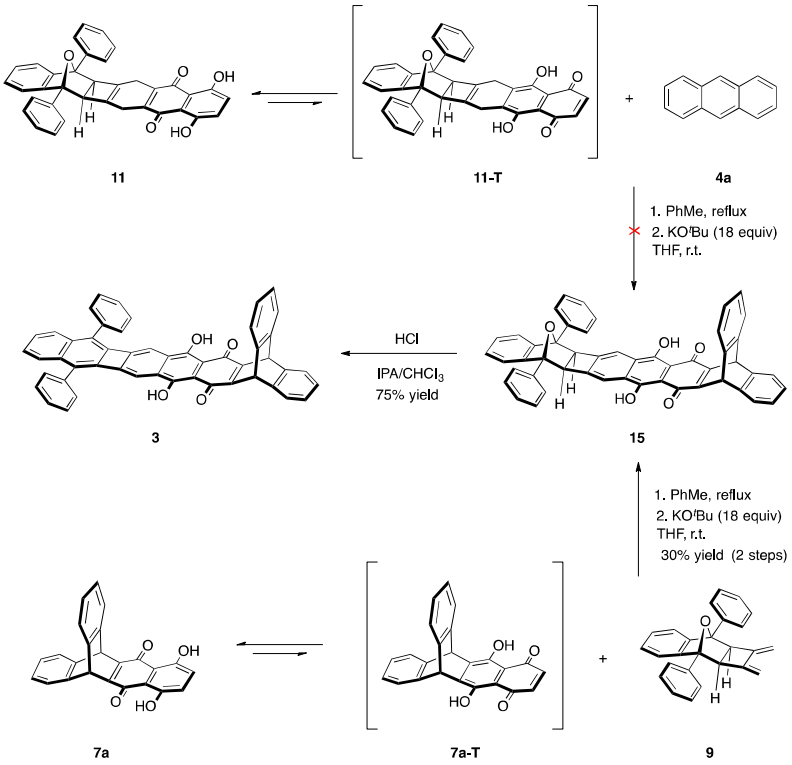

Due to the insufficient reactivity of **11-T**, we sought to access target compound **3** by reversing our synthetic strategy. To this end, we were able to successfully react **7a** with diene **9** to yield double-adduct POA-iptycene **15** in 30% yield over two steps. The final product **3** could be accessed under acidic conditions and collected in 75% yield as a dark-orange product. This compound proved reasonably soluble in 1,1,2,2-tetrachloroethane and could be characterized, but was exemplary of the solubility challenges faced in trying to access the symmetrical double POA adduct.

Spectroscopic Properties of mono- and double-adducts

The UV/vis spectra of four selected naphthazarin derivatives **1a**, **2a**, **3**, and **7a** are shown in Figure 3a (See Figures S12–22 in the SI for the UV/vis spectra of all compounds). The UV/vis spectra of **1a**, **2a**, **3**, and **7a** are characteristic of naphthazarins, showing vibronically coupled bands with significant fine structures at lower energy. The deep red-colored compound **7a** exhibits a fine-structure absorption band at λ_{max} = 568 nm (2.18 eV, ε = 4800 M^{-1} cm^{-1}). The additional triptycene unit in **1a** caused a bathochromic shift of 8 nm [λ_{max} = 576 nm (2.15 eV, ε = 6900 M^{-1} cm^{-1})].

Vertical optical transitions were calculated on the optimized structures of **7a** and **1a** by time-dependent density functional theory (TD-DFT), using the software package Gaussian 03 (See Supporting Information for further details).[42] The computed transition energies in both cases are slightly lower than the experimental values (Table S1 and S2). The spectra of mono and double POA-naphthazarin compounds **2a** and **3** display low energy bands at λ_{max} = 551 nm (2.25 eV, ε = 3180 M^{-1} cm^{-1}) and λ_{max} = 557 nm (2.23 eV, ε = 3745 M^{-1} cm^{-1}), respectively. Electrochemical analysis of these compounds reveals two quasireversible waves, consistent with literature studies (see Figure S114 and Table S5).[43,44]

Figure 3. (a) UV/vis spectra of selected compounds **1a** (red line), **2a** (black line), **3** (green line), and **7a** (blue line) in CH_2Cl_2 at 298 K. (b) Normalized absorbance (solid lines) and fluorescence (dashed lines) spectra of selected compounds **6a** (red lines, λ_{ex} = 355 nm), **8a** (blue lines, λ_{ex} = 355 nm), and **10** (green lines, λ_{ex} = 375 nm) in CH_2Cl_2 at 298 K.

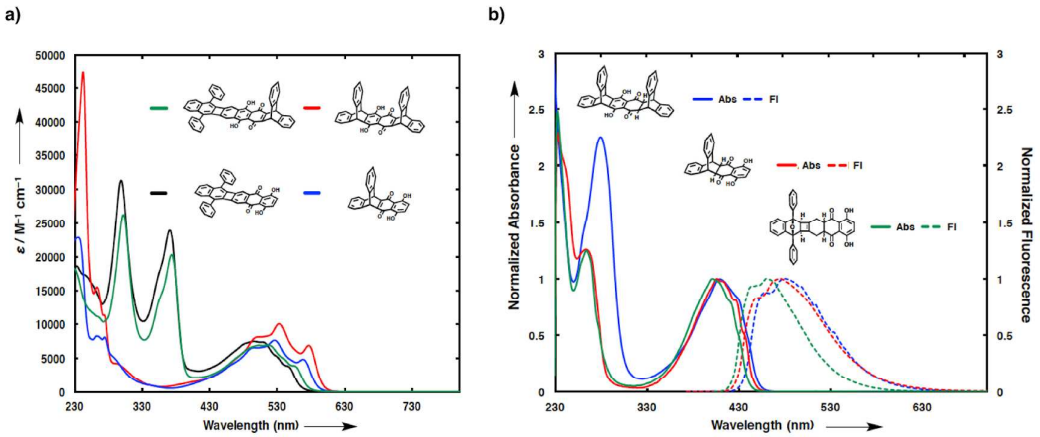

Upon analysis, some of the compounds synthesized in this study showed interesting fluorescent properties (Table 1 and Figure 3b). The unoxidized cycloaddition adducts (compounds **6a**–**d**, **8a**–**d**, and **10**) showed strong blue fluorescence with high quantum yields (Φ_F = 0.58–0.91). Though fluorescent Diels–Alder adducts of naphthazarin have been reported,[45,46] the strong fluorescence of **6a**–**d**, **8a**–**d**, and **10** was unexpected due to the lack of π-conjugation across the backbone. This strong blue emission was observed across the series, suggesting it may be due to the enolizable nature or the hydrogen-bonding capabilities of the unoxidized naphthazarin adduct.

Table 1. Photophysical characterization of emissive compounds synthesized. All measurements were performed in CH_2Cl_2 (λ_{ex} = 375 nm).

Entry	Compound	λ_{max} (nm)	ε ($M^{-1}cm^{-1}$)	λ_{em} (nm)	Φ_{em}
1	**6a**	432	3860	471	0.69
2	**6b**	434	2926	473	0.71
3	**6c**	432	3898	465	0.70
4	**6d**	435	3495	473	0.73
5	**8a**	429	4503	481	0.58
6	**8b**	433	8708	479	0.71
7	**8c**	431	6640	478	0.64
8	**8d**	434	7830	485	0.63
9	**10**	421	4804	458	0.91

Investigation of BF_2-complexation with the naphthazarin-cores Complexation of BF_3-OEt_2 with the naphthazarin core of various synthesized compounds renders the molecules fully conjugated, and was explored for potential n-type semiconducting applications.

Representative complexation studies were conducted with ^{1}H NMR, UV/vis and mass spectroscopy. For example, we were able to observe the conversion of compound **1a** to **BF_2-1a** following the addition of BF_3-OEt_2 to **1a** in CH_2Cl_2. The product could be isolated through precipitation and was analyzed by ^{1}H NMR as shown in Figure 4. Here, we observe the disappearance of the hydroxyl peak around 12 ppm, and see a distinct shift in the aromatic and bridgehead peaks upon complexation. Finally, a mixture of the two products clearly demonstrates the appearance of two discrete molecules in solution. The structure of **BF_2-1a** was also confirmed by HR-ESI-MS (*m/z* calcd for $C_{38}H_{20}B_2F_4O_4^-$: 638.1518; found: 638.1503 $[M]^-$) Susceptibility to hydrolysis was consistent with previous reports in the literature.[28,29] Presumably due to moisture present in the air, hydrolysis was observed for **BF_2-1a** to occur in $CDCl_3$ over 1-2 hours, precluding ^{13}C NMR analysis.

Figure 4. ^{1}H NMR spectra (400 MHz) of compounds **1a** to BF_2-**1a** in $CDCl_3$ at 298 K demonstrating BF_2-complexation.

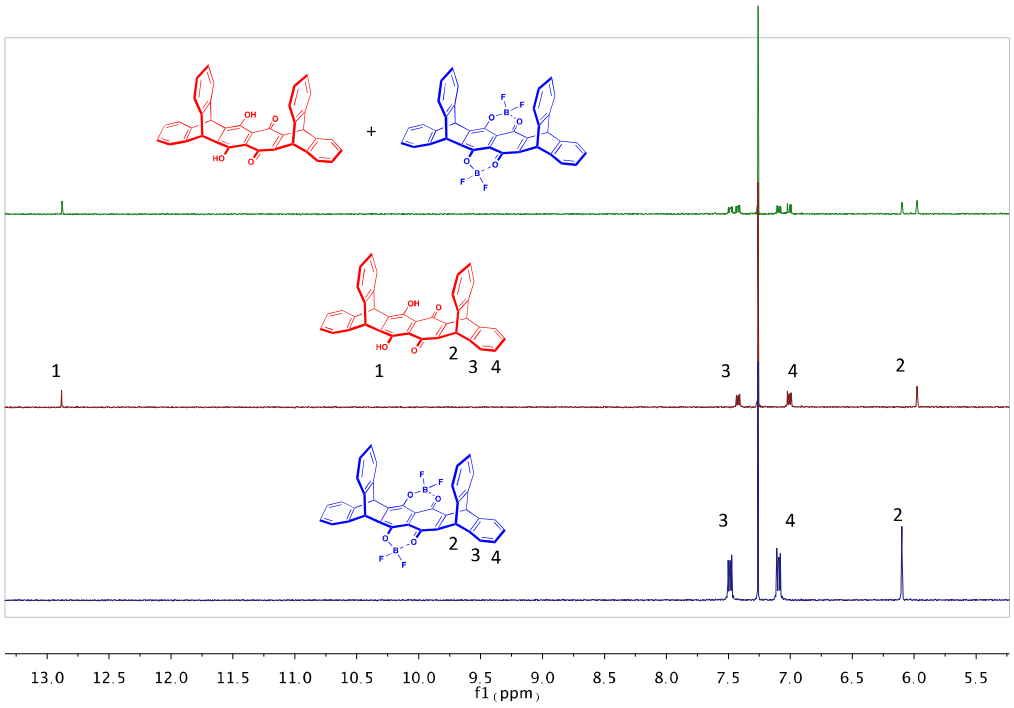

During the reaction of compound **1a** with BF_3-OEt_2, the solution changed from dark red to dark purple, and was observed by UV/vis spectroscopy as a shift in absorbance bands from ~533 nm to ~561 nm (Figure 5). This red-shifted absorption maximum of **BF_2-1a** reveals the generation of a fully conjugated structure through BF_2 chelation. Similar spectral changes were observed with **BF_2-1b** and **BF_2-1c** (see Figures S39–42 in the SI for the UV/vis spectra of **BF_2-1b** and **BF_2-1c**). In studying this complexation spectroscopically for **BF_2-2a** and **BF_2-3**, our characterization attempts were hampered by the limited solubility of substrates **2a** and **3**, similar to that observed in literature.[28,29] Despite this challenge, we were still able to observe a color change from orange to dark blue upon addition of BF_3-OEt_2, which was similar to that observed for the **BF_2-1** series (See Figures S43–45 in the SI for the UV/vis spectra of **BF_2-2a** and **BF_2-3**).

Figure 5. UV/vis spectra of compound **1a** (black line) and **BF_2-1a** (blue line) in CH_2Cl_2 at 298 K.

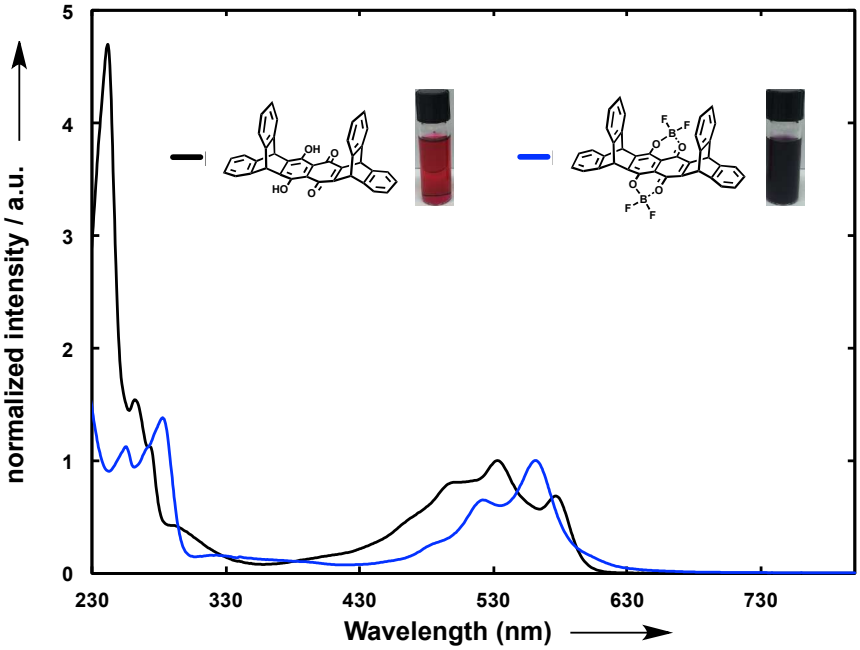
normalized intensity / a.u.
Wavelength (nm)
0
1
2
3
4
5
230
330
430
530
630
730
OH
HO
O
O
F
B
F
F

CONCLUSION

In conclusion, a selection of naphthazarin-containing polycyclic conjugated hydrocarbon molecules were synthesized and characterized, and may find utility in optoelectronic and other electronic applications. The molecular design includes 1) iptycene wings to add free space around the chromophores for better solubility, and 2) structural motifs of POAs to achieve improved stability. Successful coordination with BF_2 as a proof-of-concept reveals the potential for new conjugated n-type electronic materials or expanded coordination complex structures, such as conducting metallopolymers.

Experimental Section

General. Reagents were purchased as reagent grade and used without further purification. All solvents were of ACS reagent grade or better. Toluene was passed through a solvent purification system *via* columns of activated alumina, and stored over 3 Å sieves. Reactions in the absence of air and moisture were performed in oven-dried glassware under Ar or N_2 atmosphere. Flash column chromatography (FC) was performed using SiO_2 (60 Å, 230–400 mesh, particle size 0.040–0.063 mm) at 25 °C with a head pressure of 0.0–0.5 bar. The used solvent compositions are reported individually in parentheses. Analytical thin layer chromatography (TLC) was performed on sheets coated with silica gel (200 μm, IB-F). Visualization was achieved using UV light (254 or 366 nm). Evaporation *in vacuo* was performed at 25–60 °C and 900–10 mbar. Reported yields refer to spectroscopically and chromatographically pure compounds that were dried under high vacuum (0.1–0.05 mbar) before analytical characterization. ^{1}H and ^{13}C nuclear magnetic resonance (NMR) spectra were recorded at 500 or 400 MHz (^{1}H) and 125 or 100 MHz (^{13}C),

respectively. Chemical shifts δ are reported in ppm downfield from tetramethylsilane using the residual solvent signals as an internal reference ($CDCl_3$: δ_H = 7.26 ppm, δ_C = 77.16 ppm / $Cl_2CDCDCl_2$: δ_H = 6.0 ppm, δ_C = 73.78 ppm). For ^{1}H NMR, coupling constants *J* are given in Hz and the resonance multiplicity is described as s (singlet), d (doublet), t (triplet), q (quartet), quint (quintet), sext (sextet), sept (septet), m (multiplet), and br. (broad). All spectra were recorded at 298 K. High-resolution mass spectrometry (HRMS) was performed by the MS-service of the MIT Department of Chemistry Instrumentation Facility using an Ion Cyclotron Resonance Mass Spectrometer with either electrospray (ESI) or Direct Analysis in Real Time (DART) as the ionization technique. Where noted, additional mass spectra were obtaining using Matrix-Assisted Laser Desorption/Ionization-Time-of-Flight (MALDI-TOF)), by depositing samples directly onto the target without a matrix. UV/vis spectroscopy was recorded on a UV/vis spectrophotometer and corrected for background signal with a solvent-filled cuvette. Fluorescence spectra were measured using right-angle detection. Absolute quantum yield measurements were carried out using an integrating sphere, which was coupled to the fluorometer *via* an optical fiber bundle. Samples were excited with a 450W Xenon short arc lamp and fluorescence was detected with a detector. All photophysical measurements were performed with spectral grade dichloromethane.

Naphthazarin (**5**) was used without further purification. Anthracene (**4a**) was recrystallized from ethanol/toluene prior to use. Compounds **4b** (2,3,6,7-tetramethylanthracene),[47] **4c** (2,6-di-*tert*-butylanthracene),[48] **4d** (1,1,4,4,8,8,11,11-Octamethyl-1,2,3,4,8,9,10,11-octahydro-pentacene),[49] and diene **9**[11] were synthesized according to literature procedures.

Monoadduct triptycene synthesis: Compounds 6a–d

Naphthazarin (**5**) (1 equiv.) and the appropriate anthracene **4a**–**d** (1 equiv.) were added to a flame-dried Schlenk flask with stirrer bar, and were dissolved in the minimal amount of anhydrous toluene (1-2 mL). The headspace was purged with argon for 30 minutes, then heated to reflux overnight (111 °C). The solvent was concentrated *in vacuo*. FC (SiO_2; CH_2Cl_2, or hexanes then CH_2Cl_2 in scenarios where separation was poor) gave target adducts **6a**–**d**.

Compound 6a

Naphthazarin (**5**) (200 mg, 1.05 mmol), anthracene **4a** (188 mg, 1.05 mmol), FC (CH_2Cl_2): **6a**, yellow solid (241 mg, 62% yield). Mp: 228–230 ^oC. R_f = 0.66 (CH_2Cl_2). ^1H NMR (400 MHz, $CDCl_3$): δ 12.43 (s, 2H), 7.45 (br. dd, 2H, J = 5.4, 3.4 Hz), 7.21 (br. dd, 2H, J = 5.4, 3.4 Hz), 7.15 (br. t, 2H, J = 4.4 Hz), 7.10 (s, 2H), 6.95 (br. t, 2H, J = 4.4 Hz), 5.04 (s, 2H), 3.35 ppm (br. s, 2H). ^{13}C NMR (101 MHz, $CDCl_3$): δ 202.2, 155.8, 141.9, 139.8, 128.7, 126.9, 124.6, 124.1, 114.2, 49.63, 49.55 ppm. UV/vis (CH_2Cl_2): λ_{max} (ε) = 258 (9371), 402 (7438), 424 (5973), 432 nm (3860 M^{-1} cm^{-1}). HR-DART-MS: *m/z* calcd for $C_{24}H_{15}O_4^-$: 367.0976; found: 367.0970 $[M - H]^-$.

Compound 6b

Naphthazarin (**5**) (200 mg, 1.05 mmol), anthracene **4b** (247 mg, 1.05 mmol), FC (CH_2Cl_2): **6b**, yellow solid (205 mg, 53% yield). Mp: 206–208 ^oC. R_f = 0.74 (CH_2Cl_2). ^1H NMR (400 MHz, $CDCl_3$): δ 12.48 (s, 2H), 7.19 (s, 2H), 7.10 (s, 2H), 6.88 (s, 2H), 4.89 (s, 2H), 3.31 (s, 2H), 2.23 (s, 6H), 2.02 ppm (s, 6H). ^{13}C NMR (101 MHz, $CDCl_3$): δ 202.6, 155.8, 140.0, 137.7, 134.7, 128.5, 125.7, 125.2, 114.4, 50.0, 48.6, 19.7, 19.6 ppm (13 of 14 signals expected). UV/vis (CH_2Cl_2): λ_{max} (ε) = 263 (9368), 402 (6465), 425 (4931), 434 nm (2926 M^{-1} cm^{-1}). HR-DART-MS: *m/z* calcd for $C_{28}H_{23}O_4^-$: 423.1602; found: 423.1617 $[M - H]^-$.

Compound 6c

Naphthazarin (**5**) (100 mg, 0.53 mmol), anthracene **4c** (153 mg, 0.53 mmol), FC (100% *n*-hexanes to 100% CH_2Cl_2): **6c**, yellow solid (51 mg, 20% yield). Mp: 81–83 ^oC. R_f = 0.48 (CH_2Cl_2). ^1H NMR (400 MHz, $CDCl_3$): δ 12.30 (s, 1H), 12.26 (s, 1H), 7.47 (s, 1H), 7.37 (d, 1H, J = 7.8 Hz), 7.23 (d, 1H, J = 7.7 Hz), 7.14 (s, 1H), 7.05 – 6.99 (m, 3H), 6.91 (d, 1H, J = 7.8 Hz), 4.94 (s, 1H), 4.91 (s, 1H), 3.32 (s, 2H), 1.32 (s, 9H), 1.10 ppm (s, 9H). ^{13}C NMR (101 MHz, $CDCl_3$): δ 202.88, 202.86, 155.4, 155.3, 150.1, 150.0, 141.6, 139.5, 138.5, 136.6, 128.24, 128.19, 124.0, 123.7, 123.5, 123.3, 121.7, 121.2, 114.40, 114.36, 50.5, 50.3, 50.2, 50.0, 34.9, 34.6, 31.7, 31.4 ppm. UV/vis (CH_2Cl_2): λ_{max} (ε) = 260 (12872), 403 (7475), 432 nm (3898 M^{-1} cm^{-1}). HR-DART-MS: *m/z* calcd for $C_{32}H_{31}O_4^-$: 479.2228; found: 479.2223 $[M - H]^-$.

Compound 6d

Naphthazarin (**5**) (100 mg, 0.53 mmol), anthracene **4d** (210 mg, 0.56 mmol): **6d**, yellow solid (247 mg, 80%). Mp: 260–262 ^oC (decomp.). R_f = 0.83 (CH_2Cl_2). ^1H NMR (400 MHz, $CDCl_3$): δ 12.14 (s, 2H), 7.34 (s, 2H), 7.02 (s, 2H), 6.98 (s, 2H), 4.77 (s, 2H), 3.28 (quasi t, 2H), 1.70 – 1.62 (m, 4H), 1.49 – 1.38 (m, 4H), 1.33 (s, 6H), 1.22 (s, 6H), 1.11 (s, 6H), 0.96 ppm (s, 6H). ^{13}C NMR (101 MHz, $CDCl_3$): δ 203.5, 154.9, 143.33, 143.26, 138.3, 136.4, 127.9, 122.5, 122.0, 114.6, 50.9, 50.4, 35.3, 35.0, 34.5, 34.1, 32.19, 32.15, 31.8, 31.6 ppm. UV/vis (CH_2Cl_2): λ_{max} (ε) = 263 (11458), 403 (7872), 427 (5724), 435 nm (3495 M^{-1} cm^{-1}). HR-DART-MS: *m/z* calcd for $C_{40}H_{43}O_4^-$: 587.3167; found: 587.3142 $[M - H]^-$.

Oxidation to conjugated triptycene monoadducts: Compounds 7a–d.

To a 25 mL round-bottom flask was added **6a–d** (1 equiv.), KO^{t}Bu (6 equiv.), and 20 mL THF. After stirring under ambient conditions for 1–3 h, the blue reaction mixture was poured over NH_4Cl (aq) and extracted with EtOAc. The organic layer was dried with $MgSO_4$, filtered and evaporated. FC (SiO_2; CH_2Cl_2) gave **7a–d** as a red solid.

Compound 7a

6a (110 mg, 0.299 mmol), KO^{t}Bu (201 mg, 1.79 mmol): **7a**, red solid (107 mg, 98% yield). Mp: 317–319 ^{o}C. R_f = 0.75 (CH_2Cl_2). ^{1}H NMR (400 MHz, $CDCl_3$): δ 12.61 (s, 2H), 7.48 (br. dd, 4H, J = 5.3, 3.3 Hz), 7.09 (s, 2H), 7.06 (br. dd, 4H, J = 5.3, 3.3 Hz), 6.04 ppm (s, 2H). ^{13}C NMR (101 MHz, $CDCl_3$): δ 175.2, 167.0, 152.9, 143.6, 132.7, 125.9, 124.6, 111.4, 47.6 ppm. UV/vis (CH_2Cl_2): λ_{max} (ε) = 235 (22860), 262 (8250), 274 (8070), 496 (6520), 526 (7610), 568 nm (4800 M^{-1} cm^{-1}). HR-DART-MS: *m/z* calcd for $C_{24}H_{15}O_4^+$: 367.0965; found: 367.0954 $[M + H]^+$.

Compound 7b

6b (210 mg, 0.495 mmol), KO^{t}Bu (333 mg, 2.97 mmol): **7b**, red solid (159 mg, 76% yield). Mp: 315–317 ^{o}C. R_f = 0.83 (CH_2Cl_2). ^{1}H NMR (400 MHz, $CDCl_3$): δ 12.64 (s, 2H), 7.28 (s, 4H), 7.09 (s, 2H), 5.92 (s, 2H), 2.20 ppm (s, 12H). ^{13}C NMR (101 MHz, $CDCl_3$): δ 175.7, 166.4, 153.7, 141.5, 133.7, 132.4, 125.8, 111.4, 46.7, 19.6 ppm. UV/vis (CH_2Cl_2): λ_{max} (ε) = 245 (14350), 263 (15200), 283 (10700), 489 (4810), 526 (5610), 567 nm (3570 M^{-1} cm^{-1}) HR-DART-MS: *m/z* calcd for $C_{28}H_{23}O_4^+$: 423.1591; found: 423.1573 $[M + H]^+$.

Compound 7c

6c (40 mg, 0.083 mmol), KO^{t}Bu (56 mg, 0.499 mmol): **7c**, red solid (39 mg, 99% yield). Mp: 115–117 ^{o}C. R_f = 0.58 (DCM). ^{1}H NMR (400 MHz, $CDCl_3$): δ 12.62 (s, 2H), 7.50 (s, 2H), 7.39 (d, 2H, J = 7.9 Hz), 7.09 (s, 2H), 7.06 (d, 2H, J = 7.9 Hz), 5.97 (s, 2H), 1.26 ppm (s, 18H). ^{13}C NMR (101 MHz, $CDCl_3$): δ 176.4, 165.9, 153.7, 149.1, 143.7, 140.8, 132.3, 124.0, 122.4, 121.9, 111.5, 47.5, 34.8, 31.6 ppm. UV/vis (CH_2Cl_2): λ_{max} (ε) = 237 (13700), 260 (7590), 278 (6480), 496 (3940), 526 (4590), 568 nm (2960 M^{-1} cm^{-1}). HR-DART-MS: *m/z* calcd for $C_{32}H_{31}O_4^+$: 479.2217; found: 479.2215 $[M + H]^+$.

Compound 7d

6d (100 mg, 0.170 mmol), KO^{t}Bu (114 mg, 1.02 mmol): **7d**, red solid (85 mg, 85% yield). Mp: >350 ^{o}C R_f = 0.84 (CH_2Cl_2). ^{1}H NMR (400 MHz, $CDCl_3$): δ 12.62 (s, 2H), 7.39 (br. s, 4H), 7.05 (br. s, 2H), 5.88, (s, 2H), 1.62 (s, 8H), 1.24 ppm (s, 24H). ^{13}C NMR (101 MHz, $CDCl_3$): δ 177.8, 164.6, 154.0, 142.2, 140.6, 131.7, 122.6, 111.6, 47.1, 35.2, 34.5, 32.1, 32.0 ppm. UV/vis (CH_2Cl_2): λ_{max} (ε) = 240 (16870), 273 (12120), 284 (12600), 489 (6370), 526 (7630), 568 nm (4830 M^{-1} cm^{-1}). HR-DART-MS: *m/z* calcd for $C_{40}H_{42}O_4^+$: 587.3078; found: 587.3083 $[M + H]^+$.

Double-adduct pentiptycene synthesis: Compounds 8a–d

Compound **7a**–**d** (1 equiv.) and the appropriate anthracene **4a**–**d** (1 equiv.) were added to a flame-dried Schlenk flask with stir bar, and were dissolved in the minimal amount of anhydrous toluene (<1 mL). The headspace was purged with argon for 30 minutes, then heated to reflux overnight (111 °C). The solvent that remained was concentrated *in vacuo*. FC (SiO_2; 100% *n*-hexanes to 100% CH_2Cl_2).

Compound 8a

7a (36 mg, 0.098 mmol), **4a** (17.5 mg, 0.098 mmol): **8a**, yellow solid (22 mg, 41% yield). Mp: 190–192 ^{o}C (decomp). R_f = 0.89 (CH_2Cl_2). ^{1}H NMR (400 MHz, $CDCl_3$): δ 12.75 (s, 2H), 7.50 – 7.35 (m, 6H), 7.17 (quasi t, 2H, J = 4.3 Hz), 7.12 (quasi t, 2H, J = 4.3 Hz), 7.06 – 7.01 (m, 2H), 7.01 – 6.97 (m, 2H), 6.91 – 6.86 (m, 2H), 5.99 (s, 2H), 5.05 (s, 2H), 3.27 ppm (s, 2H). ^{13}C NMR (101 MHz, $CDCl_3$): δ 201.9, 151.2, 145.5, 144.1, 143.8, 142.1, 140.0, 126.9, 126.7, 125.74, 125.72, 124.6, 124.4, 124.3, 124.0, 113.1, 49.5, 48.8, 47.6 ppm. UV/vis (CH_2Cl_2): λ_{max} (ε) = 269 (13378), 408 (5423), 429 nm (4503 M^{-1} cm^{-1}). HR-DART-MS: *m/z* calcd for $C_{38}H_{23}O_4^-$: 543.1602; found: 543.1620 $[M – H]^-$.

Compound 8b

7b (127 mg, 0.301 mmol), **4b** (70 mg, 0.301 mmol): **8b**, yellow solid (94 mg, 48% yield). Mp: 249–251 °C. R_f = 0.88 (CH_2Cl_2). ^{1}H NMR (400 MHz, $CDCl_3$): δ 12.72 (s, 2H), 7.22 (s, 2H), 7.17 (s, 2H), 7.14 (s, 2H), 6.82 (s, 2H), 5.85 (s, 2H), 4.87 (s, 2H), 3.21 (s, 2H), 2.20 (s, 6H), 2.16 (s, 6H), 2.12 (s, 6H), 1.91 ppm (s, 6H). ^{13}C NMR (101 MHz, $CDCl_3$): δ 202.3, 150.9, 146.0, 142.0, 141.8, 140.2, 137.7, 134.8, 134.5, 133.7, 133.6, 125.7, 125.6, 125.1, 113.3, 50.0, 48.0, 46.6, 19.7, 19.6, 19.5 ppm (21 out of 23 signals expected). UV/vis (CH_2Cl_2): λ_{max} (ε) = 279 (27051), 409 (11980), 433 nm (8708 M^{-1} cm^{-1}). HR-DART-MS: *m/z* calcd for $C_{46}H_{40}O_4Na^+$: 679.2819; found: 679.2826 $[M + Na]^+$.

Compound 8c

7c (40 mg, 0.084 mmol), **4c** (24 mg, 0.084 mmol): **8c**, yellow solid (21 mg, 31% yield). Mp: 220–222 °C (decomp.). R_f = 0.71 (CH_2Cl_2). Note that by NMR we observe 4 isomers in a 1:1:1:1 ratio, based on the hydroxyl peak integration in the ^{1}H NMR spectrum.

^{1}H NMR (400 MHz, $CDCl_3$): δ 12.59 (s, 2H), 12.57 (s, 2H), 12.55 (s, 2H), 12.54 (s, 2H), 7.43 (m, 12H), 7.36 (br. s, 2H), 7.31 (m, 12H), 7.20 (br. d, *J* = 1.86 Hz, 2H), 7.18 (br. d, *J* = 1.86 Hz, 2H), 7.05 (m, 4H), 7.02 (m, 2H), 6.98 (m, 8H), 6.74 (dd, *J* = 7.82, 2.01 Hz, 2H), 6.69 (dd, *J* = 7.82, 2.01 Hz, 2H), 5.88 (m, 8H), 4.90 (m, 8H), 3.23 (m, 8H), 1.29 (m, 36H), 1.26 (m, 36H), 1.22 (m, 36H), 0.87 (s, 18H), 0.84 (s, 18H). ^{13}C NMR (101 MHz, $CDCl_3$): δ 202.73, 202.68, 150.6, 150.55, 150.53, 150.4, 149.9, 149.83, 149.78, 148.8, 148.7, 145.7, 145.6, 144.23, 144.17, 143.8, 143.7, 141.7, 141.6, 141.4, 141.3, 140.9, 139.5, 139.4, 138.84, 138.77, 136.7, 123.9, 123.7, 123.6, 123.5, 123.4, 123.1, 123.0, 122.4, 122.19, 122.17, 121.8, 121.6, 121.4, 121.2, 121.1, 113.2, 113.12, 113.07, 50.1, 50.0, 49.9, 49.8, 47.4, 36.8, 34.84, 34.75, 34.4, 34.3, 31.69, 31.65, 31.59, 31.2. UV/vis (CH_2Cl_2): λ_{max} (ε) = 275 (21100), 410 (8330), 431

nm (6640 M^{-1} cm^{-1}). HR-ESI-MS: *m/z* calcd for $C_{54}H_{56}O_4Na^+$: 791.4071; found: 791.4055 $[M + Na]^+$.

Compound 8d

7d (61 mg, 0.104 mmol), **4d** (41 mg, 0.104 mmol): **8d**, yellow solid (62 mg, 61%). Mp: > 350 °C. R_f = 0.97 (CH_2Cl_2). ^1H NMR (400 MHz, $CDCl_3$): δ 12.42 (s, 2H), 7.31 (s, 4H), 7.27 (s, 2H), 6.89 (s, 2H), 5.77 (s, 2H), 4.72 (s, 2H), 3.18 (s, 2H), 1.70 – 1.60 (m, 8H), 1.57 (s, 4H), 1.40 – 1.10 (m, 38H), 1.00 (s, 6H), 0.74 (m, 2H), 0.62 ppm (s, 6H). ^{13}C NMR (101 MHz, $CDCl_3$): δ 203.6, 150.1, 145.5, 143.2, 143.0, 141.7, 141.5, 140.6, 138.1, 136.2, 128.4, 122.5, 122.4, 122.1, 122.0, 113.0, 51.1, 50.4, 47.0, 35.4, 35.3, 34.6, 34.46, 34.45, 34.4, 33.9, 32.5, 32.2, 32.1, 32.0, 31.9, 31.8, 31.50 ppm. UV/vis (CH_2Cl_2): λ_{max} (ε) = 279 (25616), 411 (10015), 434 nm (7830 M^{-1} cm^{-1}). HR-ESI-MS: *m/z* calcd for $C_{70}H_{80}O_4Na^+$: 1007.5949; found: 1007.5963 $[M + Na]^+$.

Oxidation to conjugated pentiptycene double-adducts 1a–c.

To a 25 mL round-bottom flask was added **8a**–**c** (1 equiv.), KO^{t}Bu (6 equiv.), and 20 mL THF. After stirring under ambient conditions for 1–3 h, the blue reaction mixture was poured over NH_4Cl (aq) and extracted with EtOAc. The organic layer was dried with $MgSO_4$, filtered and evaporated. FC (SiO_2; CH_2Cl_2) gave **1a**–**d** as a red solid.

Compound 1a

8a (55 mg, 0.101 mmol), KO^{t}Bu (68 mg, 0.606 mmol): **1a**, red solid (38 mg, 69% yield). Mp: >350 °C. R_f = 0.91 (CH_2Cl_2). ^1H NMR (400 MHz, $CDCl_3$): δ 12.88 (s, 2H), 7.42 (br. dd, 8H, J = 5.3, 3.2 Hz), 7.01 (br. dd, 8H, J = 5.3, 3.2 Hz), 5.98 ppm (s, 4H). ^{13}C NMR (101 MHz, $CDCl_3$): δ 169.1, 151.1, 143.7, 125.8, 124.5, 110.2, 47.6 ppm. UV/vis (CH_2Cl_2): λ_{max} (ε) = 242 (47370), 262 (15520), 291 (4270), 502 (8140), 533 (10070), 576 nm (6900 M^{-1} cm^{-1}). HR-DART-MS: *m/z* calcd for $C_{38}H_{23}O_4^+$: 543.1591; found: 543.1583 $[M + H]^+$.

Compound 1b

8b (94 mg, 0.143 mmol), KO^{t}Bu (96 mg, 0.859 mmol): **1b**, red solid (51 mg, 54% yield). Mp: >350 ^{o}C. R_f = 0.80 (CH_2Cl_2). ^{1}H NMR (400 MHz, $CDCl_3$): δ 12.87 (s, 2H), 7.18 (s, 8H), 5.82 (s, 4H), 2.13 ppm (s, 24H). ^{13}C NMR (101 MHz, $CDCl_3$): δ 169.0, 151.6, 141.7, 133.5, 125.7, 110.1, 46.7, 19.6 ppm. UV/vis (CH_2Cl_2): λ_{max} (ε) = 248 (30200), 273 (20415), 283 (17150), 502 (7500), 534 (9160), 577 nm (6420 M^{-1} cm^{-1}). HR-DART-MS: *m/z* calcd for $C_{46}H_{39}O_4^+$: 655.2843; found: 655.2856 $[M + H]^+$.

Compound 1c

8c (111 mg, 0.144 mmol), KO^{t}Bu (97 mg, 0.866 mmol): **1c**, red solid (50 mg, 45% yield). Mp: 264–266 ^{o}C. R_f = 0.97 (CH_2Cl_2). ^{1}H NMR (400 MHz, $CDCl_3$): δ 12.95 (s, 2H), 7.46 (s, 4H), 7.36 (br. d, 4H, J = 7.7 Hz), 7.03 (br. d, 4H, J = 7.7 Hz), 5.94 (s, 4H), 1.25 ppm (s, 36H). ^{13}C NMR (101 MHz, $CDCl_3$): δ 169.2, 151.6, 148.9, 143.8, 140.9, 123.8, 122.3, 121.7, 110.1, 47.5, 34.8, 31.6 ppm. UV/vis (CH_2Cl_2): λ_{max} (ε) = 245 (41075), 267 (19620), 278 (15230), 504 (8130), 533 (10010), 577 nm (6910 M^{-1} cm^{-1}). HR-ESI-MS: *m/z* calcd for $C_{54}H_{55}O_4^+$: 767.4095; found: 767.4088 $[M + H]^+$.

Synthesis of the POA series

Compound 10

Naphthazarin (**5**) (100 mg, 0.526 mmol) and diene **9** (238 mg, 0.684 mmol) were added to either an oven-dried pressure tube or flame-dried Schlenk flask with stirrer bar, and were dissolved in the minimal amount of anhydrous toluene (1–2 mL). The headspace was purged with argon for 30 minutes, then heated to reflux overnight (111 °C). The solvent was concentrated *in vacuo*. Gravity column chromatography (SiO_2: CH_2Cl_2) or FC (SiO_2; 100% *n*-hexanes to 100% CH_2Cl_2) yielded 138 mg (49% yield) of a yellow solid. Note that while the highest yields were obtained when carried out in

a pressure tube, similar yields are obtained when carried out under refluxing conditions. Note also that by NMR we observe 1:0.20:0.20 ratio of isomers, based on the hydroxyl peaks. The ^{1}H NMR integrations are calculated such that hydroxyl peaks in 11.94–11.79 integrate to a total of 2H. Mp: 301–303 ^{o}C. R_f = 0.32 (DCM). ^{1}H NMR (400 MHz, $CDCl_3$): δ 11.94 (s, 0.28 H), 11.90 (s, 0.28 H), 11.78 (s, 1.43 H), 7.66 (m, 4 H), 7.44 (m, 6 H), 7.20 (s, 2 H), 7.12 (m, 2 H), 6.95 (m, 2 H), 3.47 (m, 2 H), 3.13 (m, 2 H), 2.20 (m, 4 H). ^{13}C NMR (101 MHz, $CDCl_3$): δ 203.5, 202.7, 155.3, 155.2, 155.1, 148.1, 140.7, 140.5, 137.2, 137.1, 128.7, 128.62, 128.57, 128.51, 128.4, 128.3, 128.2, 128.16, 128.1, 127.0, 126.9, 126.8, 119.4, 119.3, 113.4, 86.43, 86.39, 86.3, 54.0, 53.6, 53.3, 46.3, 46.0, 45.8, 25.4, 24.8, 23.7. UV/vis (CH_2Cl_2): λ_{max} (ε) = 259 (8606), 398 (6903), 421 nm (4804 M^{-1} cm^{-1}). HR-DART-MS: *m/z* calcd for $C_{36}H_{27}O_5^+$: 539.1853, found 539.1852 $[M+H]^+$.

Compound 11

To a 25 mL round-bottom flask was added **10** (330 mg, 0.613 mmol) and KO^{t}Bu (206 mg, 1.84 mmol) in 20 mL THF. The reaction was stirred under ambient conditions for 1–5 min, and was monitored by TLC for the appearance of the red partially oxidized product **11** and stopped immediately following the appearance of the orange fully oxidized **12.** The dark blue reaction mixture was poured over NH_4Cl (aq) and extracted with EtOAc. The organic layer was dried with $MgSO_4$, filtered and evaporated. FC (SiO_2; CH_2Cl_2) gave **11** as a red solid (171 mg, 52% yield). Mp: 293–295 ^{o}C. R_f = 0.40 (CH_2Cl_2). ^{1}H NMR (400 MHz, $CDCl_3$): δ 12.41 (s, 2H), 7.70 (d, 4H, *J* = 6.9 Hz), 7.50 (t, 4H, *J* = 7.4 Hz), 7.45 – 7.39 (m, 2H), 7.19 – 7.07 (m, 4H), 6.98 (dd, 2H, *J* = 5.3, 3.0 Hz), 3.62 (s, 2H), 3.18 – 3.05 (m, 2H), 2.87 – 2.74 ppm (m, 2H). ^{13}C NMR (101 MHz, $CDCl_3$): δ 186.3, 158.6, 148.1, 143.9, 138.5, 137.0, 129.6, 128.7, 128.3, 127.0, 126.8, 119.4, 111.4, 86.4, 54.0, 24.2 ppm. UV/vis (CH_2Cl_2): λ_{max}

(ε) = 279 (7718), 482 (6380), 511 (7071), 550 nm (4181 M^{-1} cm^{-1}). HR-DART-MS: *m/z* calcd for $C_{36}H_{25}O_5^+$: 537.1697; found: 537.1684 $[M + H]^+$.

Compound 12

To a 25 mL round-bottom flask was added **10** (105 mg, 0.195 mmol) and KO^{t}Bu (394 mg, 3.51 mmol) in 20 mL THF. After stirring under ambient conditions for 1–3 h, the blue reaction mixture was poured over NH_4Cl (aq) and extracted with EtOAc. The organic layer was dried with $MgSO_4$, filtered and evaporated. FC (SiO_2; CH_2Cl_2) gave **12** as an orange solid (81 mg, 78% yield). Mp: 304–305 ^oC. R_f = 0.47 (CH_2Cl_2). ^1H NMR (400 MHz, $CDCl_3$): δ 12.80 (s, 2H), 7.75 – 7.70 (m, 6H), 7.56 – 7.52 (m, 4H), 7.49 – 7.44 (m, 2H), 7.22 (dd, 2H, J = 5.4, 3.0 Hz), 7.19 (s, 2H), 7.11 (dd, 2H, J = 5.4, 3.0 Hz), 4.34 ppm (s, 2H). ^{13}C NMR (101 MHz, $CDCl_3$): δ 187.1, 157.7, 151.0, 147.5, 135.7, 134.5, 129.2, 128.9, 128.6, 127.5, 126.8, 121.2, 119.7, 112.5, 89.0, 55.7 ppm. UV/vis (CH_2Cl_2): λ_{max} (ε) = 275 (38000), 486 nm (8080 M^{-1} cm^{-1}). HR-DART-MS: *m/z* calcd for $C_{36}H_{23}O_5^+$: 535.1540; found: 535.1541 $[M + H]^+$.

Compound 2a

In a flame-dried 25 mL Schlenk flask, compound **12** (21 mg, 0.039 mmol) was dissolved in 1:1 isopropyl alcohol-$CHCl_3$ (0.5 mL each). Concentrated HCl (0.2 mL) was added slowly to the solution under argon. The solution was heated to 80 ^oC for 4 hours. The product was washed with deionized water and extracted with CH_2Cl_2, then concentrated *in vacuo*. The product was washed with hexanes, then filtered and dried overnight under vacuum, affording **2a** as a red solid (17 mg, 84% yield). Mp: > 350 ^oC. R_f = 0.53 (CH_2Cl_2). ^1H NMR (400 MHz, $CDCl_3$): δ 12.88 (s, 2H), 7.87 (dd, 2H, J = 6.3, 3.4 Hz), 7.65 – 7.60 (m, 8H), 7.56 (s, 2H), 7.55 – 7.50 (m, 2H), 7.37 (dd, 2H, J = 6.3, 3.4 Hz), 7.27 ppm (s, 2H). UV/vis (CH_2Cl_2): λ_{abs} (ε) = 298 (31300), 370

(23900), 511 (7270), 551 nm (3180 M^{-1} cm^{-1}). HR-DART-MS: *m/z* calcd for $C_{36}H_{21}O_4^+$: 517.1434; found: 517.1422 $[M + H]^+$.

Compound 2b

In a flame-dried 25 mL Schlenk flask, compound **12** (154 mg, 0.288 mmol) was dissolved in 10 mL acetic anhydride with *p*-TsOH crystals (694 mg, 4.0 mmol). The solution was heated to 120 ^oC for 12 hours. The product was precipitated by pouring solution over ice, and adding water until a solid precipitate formed. The product was filtered and dried overnight under vacuum, affording **2b** as an orange solid (100 mg, 58% yield). Mp: 285–287 ^oC. R_f = 0.33 (CH_2Cl_2). ^1H NMR (400 MHz, $CDCl_3$): δ 7.84 (dd, 2H, J = 6.2, 3.4 Hz), 7.62 – 7.57 (m, 8H), 7.55 – 7.48 (m, 2H), 7.40 – 7.32 (m, 6H), 2.45 ppm (s, 6H). ^{13}C NMR (101 MHz, $CDCl_3$): δ 183.3, 169.6, 155.7, 148.1, 142.2, 136.1, 135.7, 135.2, 131.5, 130.9, 129.6, 129.1, 128.5, 127.6, 127.4, 125.8, 115.3, 21.3 ppm. UV/vis (CH_2Cl_2): λ_{max} (ε) = 299 (41950), 368 (39395), 463 nm (2878 M^{-1} cm^{-1}). HR-DART-MS: *m/z* calcd for $C_{40}H_{25}O_6^+$: 601.1646; found: 601.1643 $[M + H]^+$.

Compound 13

11 (32 mg, 0.060 mmol) and diene **9** (21 mg, 0.060 mmol) were added to a flame-dried Schlenk flask with stir bar, and were dissolved in the minimal amount of anhydrous toluene (1–2 mL). The headspace was purged with argon for 30 minutes, then heated to reflux overnight (111 °C). The solvent was concentrated *in vacuo*. KO^{t}Bu (121 mg, 1.07 mmol) and 20 mL THF were added to the flask, and the reaction was allowed to stir 1–3 h under ambient conditions. The blue reaction mixture was then poured over NH_4Cl (aq) and extracted with EtOAc. The organic layer was dried with $MgSO_4$, filtered and evaporated. Gravity column chromatography (SiO_2: CH_2Cl_2) gave **13** (7 mg, 13% yield) as an orange solid. Mp:

315–317 °C. R_f = 0.75 (CH_2Cl_2). ^{1}H NMR (400 MHz, $CDCl_3$): δ 15.03 (s, 2H), 7.80 (s, 4H), 7.75 – 7.71 (m, 8H), 7.52 (t, 8H, J = 7.4 Hz), 7.47 – 7.42 (m, 4H), 7.20 (dd, 4H, J = 5.4, 3.0 Hz), 7.09 (dd, 4H, J = 5.4, 3.0 Hz), 4.34 ppm (s, 4H). ^{13}C NMR (100 MHz, $CDCl_3$): δ 179.6, 172.7, 148.8, 147.8, 135.9, 133.3, 128.8, 128.5, 127.4, 126.9, 120.1, 119.7, 113.6, 105.8, 89.2, 55.5 ppm. UV/vis (CH_2Cl_2): λ_{max} (ε) = 285 (76508), 491 (24618), 462 (15226), 315 (24907), 526 nm (22821 M^{-1} cm^{-1}). HR-DART-MS: *m/z* calcd for $C_{62}H_{38}O_6Na^+$: 901.2561; found: 901.2549 $[M + Na]^+$.

Compound 14

In a flame-dried 25 mL Schlenk flask, compound **13** (21 mg, 0.039 mmol) was dissolved in 1:1 isopropyl alcohol-$CHCl_3$ (0.5 mL each). Concentrated HCl (0.2 mL) was added slowly to the solution under argon. The solution was heated to 80 °C for four hours. The product was washed with deionized water and extracted with CH_2Cl_2, then concentrated *in vacuo*, affording insoluble dark colored solid. Poor solubility and decomposition precluded further characterization beyond mass detection by MALDI-TOF. MALDI-TOF-MS: *m/z* calcd for $C_{62}H_{34}O_4^+$: 842.24, found 842.08 $[M]^+$ (See S112–113. for mass spectrum).

Iptycene-POAs

Compound 15

7a (90 mg, 0.246 mmol) and diene **9** (86 mg, 0.246 mmol) were added to a flame-dried Schlenk flask with stir bar, and were dissolved in the minimal amount of anhydrous toluene (1–2 mL). The headspace was purged with argon for 30 minutes, then heated to reflux overnight (111 °C). The solvent was concentrated *in vacuo*. KO^{t}Bu (496 mg, 4.42 mmol) and 20 mL THF were added to the flask, and the reaction was allowed to stir 1–3 h under ambient conditions. The blue reaction mixture was then poured over NH_4Cl (aq) and extracted with EtOAc. The organic

layer was dried with $MgSO_4$, filtered and evaporated. Gravity column (SiO_2: CH_2Cl_2) or FC (SiO_2; hexanes then CH_2Cl_2) yielded an orange solid **15** (53 mg, 30% yield). Mp: 251–253 °C. R_f = 0.88 (CH_2Cl_2). ^{1}H NMR (400 MHz, $CDCl_3$): δ 13.13 (s, 2H), 7.72 (d, 4H, J = 6.9 Hz), 7.69 (s, 2H), 7.52 (t, 4H, J = 7.4 Hz), 7.49 – 7.41 (m, 6H), 7.20 (dd, 2H, J = 5.4, 3.0 Hz), 7.08 (dd, 2H, J = 5.4, 3.0 Hz), 7.05 – 6.99 (m, 4H), 6.07 (s, 2H), 4.31 ppm (s, 2H). ^{13}C NMR (101 MHz, $CDCl_3$): δ 180.2, 153.3, 150.6, 147.6, 146.2, 144.2, 144.0, 135.7, 134.6, 128.9, 128.6, 127.5, 126.8, 125.8, 125.7, 124.5, 124.4, 121.2, 119.7, 111.2, 89.0, 55.6, 47.6 ppm. UV/vis (CH_2Cl_2): λ_{max} (ε) = 280 (68245), 494 (13190), 529 nm (7575 M^{-1} cm^{-1}). HR-DART-MS: *m/z* calcd for $C_{50}H_{29}O_5^-$: 709.2020; found: 709.2000 $[M - H]^-$.

Compound 3

In a flame-dried 25 mL Schlenk flask, compound **15** (22 mg, 0.031 mmol), was dissolved in 1:1 isopropyl alcohol-$CHCl_3$ (0.5 mL each). Concentrated HCl (0.2 mL) was added slowly to the solution under argon. The solution was heated to 80 °C for 4 hours. The product was washed with deionized water and extracted with CH_2Cl_2, then concentrated *in vacuo*. The product was washed with hexanes, then filtered and dried overnight under vacuum, affording **3** as an orange solid (16 mg, 75% yield). Mp: >350 °C. R_f = 0.95 (CH_2Cl_2). ^{1}H NMR (500 MHz, 1,1,2,2-tetrachloroethane-d_2): δ 13.10 (s, 2H), 7.84 (dd, 2H, J = 6.3, 3.4 Hz), 7.64 – 7.59 (m, 8H), 7.58 – 7.50 (m, 6H), 7.49 (s, 2H), 7.32 (dd, 2H, J = 6.3, 3.4 Hz), 7.09 (dd, 4H, J = 5.5, 3.1 Hz), 6.11 ppm (s, 2H). ^{13}C NMR (125 MHz, 1,1,2,2-tetrachloroethane-d_2): δ 186.0, 155.8, 153.1, 146.0, 143.7, 141.7, 135.8, 135.1, 134.7, 131.3, 129.3, 128.9, 128.4, 127.34, 127.30, 125.6, 124.4, 114.9, 110.7, 47.2 ppm. UV/vis (CH_2Cl_2): λ_{max} (ε) = 301 (26248), 373, (20280), 517 (6910), 604 nm (3745 M^{-1} cm^{-1}). MALDI-TOF-MS: *m/z*

calcd for $C_{50}H_{29}O_5^-$: 692.20; found: 692.538 $[M]^+$. HR-DART-MS: *m/z* calcd for $C_{50}H_{29}O_4^+$: 693.2060; found: 693.2050 $[M + H]^+$.

Synthesis of BF_2 complexes

Naphthazarin derivative (20 mg) was added to a flame-dried Schlenk flask with stirrer bar, and were dissolved in dry CH_2Cl_2 (5 mL) and BF_3-OEt_2 (0.5 mL). The headspace was purged with argon, then stirred at room temperature for 1 h. The solvent was concentrated *in vacuo*. The product was washed with hexanes and dried overnight under vacuum, affording BF_2 complexes.

Compound 1a-BF_2

1a (20 mg, 0.037 mmol): **1a-BF_2**, dark purple solid (18 mg, 77% yield). R_f = 0.89 (CH_2Cl_2). ^{1}H NMR (300 MHz, $CDCl_3$): δ 7.49 (br. dd, 8H, J = 5.4, 3.2 Hz), 7.09 (br. dd, 8H, J = 5.4, 3.2 Hz), 6.10 ppm (s, 4H). HR-ESI-MS: *m/z* calcd for $C_{38}H_{20}B_2F_4O_4^-$: 638.1518; found: 638.1503 $[M]^-$.

ASSOCIATED CONTENT

Supporting Information.

^{1}H and ^{13}C NMR spectra of all new compounds, crystal structure data for compounds **6b**, **7a**, **8a**, **10**, **11**, and **12**, UV/vis and fluorescence characterization, and TD-DFT calculations can be found in the Supporting Information for this manuscript. This material is available free of charge via the Internet at http://pubs.acs.org.

AUTHOR INFORMATION

Corresponding Author

*E-mail: tswager@mit.edu

Notes

The authors declare no competing financial interest.

[§] These two authors contributed equally to this work.

ACKNOWLEDGMENTS

This work was supported by the National Science Foundation through award DMR-1410718, and Graduate Research Fellowships (Grant No. 122374 (G. D. G. and S. P. L.) Any opinion, findings, and conclusions or recommendations expressed in this material are those of the authors(s) and do not necessarily reflect the views of the National Science Foundation. This was also supported by an Early Postdoc Mobility fellowship from the Swiss National Science Foundation (SNF) (C. D.). The authors thank Dr. Peter Müller and Dr. Jonathan Becker for collecting and solving X-ray structure data and Dr. Tristan Reekie for reviewing the manuscript.

REFERENCES

(1) Anthony, J. E. *Chem. Rev.* **2006**, *106*, 5028–5048.

(2) Anthony, J. E. *Angew. Chem. Int. Ed.* **2008**, *47*, 452–483.

(3) Mei, J.; Diao, Y.; Appleton, A. L.; Fang, L.; Bao, Z. *J. Am. Chem. Soc.* **2013**, *135*, 6724–6746.

(4) Kaur, I.; Jia, W.; Kopreski, R. P.; Selvarasah, S.; Dokmeci, R. M.; Pramanik, C.; McGruer, N. E.; Miller, G. P. *J. Am. Chem. Soc.* **2008**, *130*, 16274–16286.

(5) Laquindanum, J. G.; Katz, H. E.; Lovinger, A. J. *J. Am. Chem. Soc.* **1998**, *120*, 664–672.

(6) Engelhart, J. U.; Lindner, B. D.; Tverskoy, O.; Rominger, F.; Bunz, U. H. F. *Chem. - Eur. J.* **2013**, *19*, 15089–15092.

(7) Yang, S.; Shan, B.; Xu, X.; Miao, Q. *Chem. - Eur. J.* **2016**, *22*, 6637–6642.

(8) Appleton, A.; Barlow, S.; Marder, S.; Hardcastle, K.; Bunz, U. *Synlett* **2011**, *22*, 1983–1986.

(9) Wang, C.; Zhang, J.; Long, G.; Aratani, N.; Yamada, H.; Zhao, Y.; Zhang, Q. *Angew. Chem. Int. Ed.* **2015**, *54*, 6292–6296.

(10) Li, J.; Zhang, Q. *Synlett* **2013**, *24*, 686–696.

(11) Li, J.; Chen, S.; Wang, Z.; Zhang, Q. *Chem. Rec.* **2016**, *16*, 1518–1530.

(12) Gu, P.-Y.; Wang, Z.; Liu, G.; Yao, H.; Wang, Z.; Li, Y.; Zhu, J.; Li, S.; Zhang, Q. *Chem. Mater.* **2017**, *29*, 4172–84175.

(13) Li, J.; Zhang, Q. *ACS Appl. Mater. Interfaces* **2015**, *7*, 28049–28062.

(14) Helson, H. E.; Vollhardt, P. C.; Yang, Z.-Y. *Angew. Chem. Int. Ed.* **1985**, *24*, 114–115.

(15) Schleifenbaum, A.; Feeder, N.; Vollhardt, K. P. C. *Tetrahedron Lett.* **2001**, *42*, 7329–7332.

(16) Parkhurst, R. R.; Swager, T. M. *J. Am. Chem. Soc.* **2012**, *134*, 15351–15356.

(17) Parkhurst, R. R.; Swager, T. M. *Top. Curr. Chem.* **2014**, *350*, 141–176.

(18) Biegger, P.; Schaffroth, M.; Patze, C.; Tverskoy, O.; Rominger, F.; Bunz, U. H. F. *Chem. - Eur. J.* **2015**, *21*, 7048–7052.

(19) Luppino, S.; Swager, T. *Synlett* **2016**, *28*, 323–326.

(20) Chen, Z.; Müller, P.; Swager, T. M. *Org. Lett.* **2006**, *8*, 273–276.

(21) Miao, Q.; Chi, X.; Xiao, S.; Zeis, R.; Lefenfeld, M.; Siegrist, T.; Steigerwald, M. L.; Nuckolls, C. *J. Am. Chem. Soc.* **2006**, *128*, 1340–1345.

(22) Fukutani, T.; Hirano, K.; Satoh, T.; Miura, M. *J. Org. Chem.* **2011**, *76*, 2867–2874.

(23) Echavarren, A.; Prados, P.; Farina, F. *Tetrahedron* **1984**, *40*, 4561–4567.

(24) de Bie, J. F. M.; Peperzak, R. M.; Daenen, M. J.; Scheeren, H. W. *Tetrahedron* **1993**, *49*, 6463–6472.

(25) Kelly, T. R.; Gillard, J. W.; Goerner, R. N.; Lyding, J. M. *J. Am. Chem. Soc.* **1977**, *99*, 5513–5514.

(26) Fariña, F.; Vega, J. C. *Tetrahedron Lett.* **1972**, *13*, 1655–1658.

(27) Carreño, M. C.; Ruano, J. L. G.; Urbano, A. *J. Org. Chem.* **1996**, *61*, 6136–6138.

(28) Ono, K.; Hashizume, J.; Yamaguchi, H.; Tomura, M.; Nishida, J. I.; Yamashita, Y. *Org. Lett.* **2009**, *11*, 4326–4329.

(29) Ono, K.; Yamaguchi, H.; Taga, K.; Saito, K.; Nishida, J. L.; Yamashita, Y. *Org. Lett.* **2009**, *11*, 149–152.

(30) Cao, J.; Zhu, X. Z.; Chen, C. F. *J. Org. Chem.* **2010**, *75*, 7420–7423.

(31) Amara, J. P.; Swager, T. M. *Macromolecules* **2004**, *37*, 3068–3070.

(32) Quinti, L.; Allen, N. S.; Edge, M.; Murphy, B. P.; Perotti, A. *J. Photochem. Photobiol. A Chem.* **2003**, *155*, 79−91.

(33) Quinti, L.; Allen, N. S.; Edge, M.; Murphy, B. P.; Perotti, A. *J. Photochem. Photobiol. A Chem.* **2003**, *155*, 93−106.

(34) Kaupp, G.; Griiter, H.-W.; Teufel, E. *Chem. Ber.* **1983**, *116*, 618–629.

(35) Huntsman, W.; Wristers, H. *J. Am. Chem. Soc.* **1963**, *85*, 3308–3309.

(36) Huntsman, W.; Wristers, H. *J. Am. Chem. Soc.* **1967**, *89*, 342–347.

(37) Blomquist, A. T.; Maitlis, P. M. *Proc. Chem. Soc.* **1961**, 332.

(38) Hopf, H. *Angew. Chem. Int. Ed.* **1970**, *9*, 732–732.

(39) Toda, F.; Garratt, P. *Chem. Rev.* **1992**, *92*, 1685–1707.

(40) Sauer, J.; Sustmann, R. *Angew. Chem. Int. Ed.* **1980**, *19*, 779–807.

(41) Jin, Z.; Teo, Y. C.; Zulaybar, N. G.; Smith, M. D.; Xia, Y. *J. Am. Chem. Soc.* **2017**, *139*, 1806–1809.

(42) Frisch, M. J.; Trucks, G. W.; Schlegel, H. B.; Scuseria, G. E.; Robb, M. A.; Cheeseman, J. R.; Montgomery Jr., J. A.; Vreven, T.; Kudin, K. N.; Burant, J. C.; Millam, J. M.; Iyengar, S. S.; Tomasi, J.; Barone, V.; Mennuci, B.; Cossi, M.; Scalmani, G.; Rega, N.; Petersson, G. A.; Nakatsuji, H.; Hada, M.; Ehara, M.; Toyata, K.; Fukuda, R.; Hasegawa, J.; Ishida, M.; Nakajima, T.; Honda, Y.; Kitao, O.; Nakai, H.; Klene, M.; Li, X.; Knox, J. E.; Hratchian, H. P.; Cross, J. B.; Bakken, V.; Adamo, C.; Jaramillo, J.; Gomperts, R.; Stratmann, R. E.; Yazyev, O.; Austin, A. J.; Cammi, R.; Pomelli, C.; Ochterski, J. W.; Ayala, P. Y.; Morokuma, K.; Voth, G. A.; Salvador, P.; Dannenberg, J. J.; Zakrzewski, V. G.; Dapprich, S.; Daniels, A. D.; Strain, M. C.; Farkas, O.; Malick, D. K.; Rabuck, A. D.; Raghavachari, K.; Foresman, J. B.; Ortiz, J. V.; Cui, Q.; Baboul, A. G.; Clifford, S.; Cioslowski, J.; Stefanov, B. B.; Liu, G.; Liashenko, A.; Piskorz, P.; Komaromi, I.; Martin, R. L.; Fox, D. J.; Keith, T.; Al-Laham, M. A.; Peng, C. Y.; Nanayakkara, A.; Challacombe, M.; Gill, P. M. W.; Johnson, B.; Chen, W.; Wong, M. W.; Gonzalez, C.; Pople, J. A. *Gaussian*

03, revision E.01.; Gaussian, Inc.: Wallingford CT, 2004.

(43) Gomez, M.; González, F. J.; González, I. *J. Electroanal. Chem.* **2005**, *578*, 193–202.

(44) Armendariz-Vidales, G.; Frontana, C. *Org. Biomol. Chem.* **2014**, *12*, 6393–6398.

(45) Kelly, T. R.; Ananthasubramanian, L.; Borah, K.; Gillard, J. W.; Goerner, R. N.; King, P. F.; Lyding, J. M.; Tsang, W.-G.; Vaya, J. *Tetrahedron* **1984**, *40*, 4569–4577.

(46) Anathasubramanian, L.; Kelly, T. R.; Vaya, J. p-Nitrocarbobenzoxy naphthazarin. US4472312 A, 1983.

(47) Barnett, E. D. B.; Way, N. F. G.; Watson, J. W. *Ber. Dtsch. Chem. Ges.* **1933**, *66*, 1876–1891.

(48) Fu, P. P.; Harvey, R. G. *J. Org. Chem.* **1977**, *42*, 2407–2410.

(49) Bouffard, Z.; Eaton, R. F.; Müller, P.; Swager, T. M. *J. Org. Chem.* **2007**, *72*, 10166–10180.

TOC Graphic